1. INTRODUCTION

As structural analysts force the limits of their project funding and computer resources with ever larger finite element models, the topic of special matrix solution techniques becomes increasingly popular.

One such technique, known variously as static reduction, static substructuring, or the superelement method, replaces the DECOMP* and FBS* operations on a single large matrix with several smaller reductions. The reduction of a substructure to a boundary matrix, also called a superelement, is one such example. When the total structure contains identical substructures, a superelement may be reused several times.

For structures exhibiting symmetry of properties and of boundary conditions, a second technique is available to reduce the problem size. The principles of reflective symmetry, as discussed in Section 2 of this paper, enable the analyst to reduce the size of his finite element model by one-half for each plane of symmetry in the structure.

Having introduced the concepts of static reduction and symmetry transformation, we now turn our attention to certain geometries, the optimum solution of which would involve a combination of the above two techniques.

The structure shown in Figure 1 (extracted from Reference 3) has four planes of reflective symmetry; in cyclic symmetry terminology it has four segments of rotational symmetry, each with a plane of dihedral symmetry. A typical one-eighth segment finite element model of the caisson is shown in Figure 2; since it is too large for a one-step reduction to the boundaries, double stiffness reduction was necessary before cyclic transformation. This matrix technique was implemented in Reference 3 as a DMAP Alter to Rigid Format 49.

---

* NASTRAN terminology for matrix decomposition and forward-backward substitution (Reference 1, Chapter 5)

With the advent of identical superelements in NASTRAN, the structure described above becomes even easier to solve: the walls, roof and base of each caisson cell can be represented by a few typical superelements.

Another structure is shown schematically in Figure 3. Its characteristic features are several identical substructures, each having a plane of reflective symmetry. The present day NASTRAN user would be inclined to use eight mirror-image superelements; thereby saving considerable matrix reduction cost; still, the residual structure matrix is of a large enough size to necessitate multilevel reduction.

A new matrix reduction scheme for the latter structure was prompted by an intuitive feeling that the principle of symmetric components has not been taken advantage of; furthermore, that if such a scheme did exist at the substructure level, it should also allow reducing out nodes on the plane of symmetry. The rest of this paper presents the matrix equations to justify the new scheme.

2. PRINCIPLES OF REFLECTIVE SYMMETRY

Structures having an overall plane of reflective symmetry (Fig. 2) in stiffness and boundary conditions can be solved by applying the principle of decomposition of the displacement vector U into symmetric components:

$$\begin{Bmatrix} U^S \\ U^A \end{Bmatrix} = \frac{1}{2} \overbrace{\begin{bmatrix} I & I \\ I & -I \end{bmatrix}}^{\text{reflective transform}} \begin{Bmatrix} U^R \\ U^L \end{Bmatrix} \qquad (1)$$

(The symbols used in all equations are explained in the Appendix.)

The inverse transformation is:

$$\begin{Bmatrix} U^R \\ U^L \end{Bmatrix} = \begin{bmatrix} I & I \\ I & -I \end{bmatrix} \begin{Bmatrix} U^S \\ U^A \end{Bmatrix} \quad (2)$$

The same transformation can be applied to an arbitrary load vector P:

$$\begin{Bmatrix} P^R \\ P^L \end{Bmatrix} = \begin{bmatrix} I & I \\ I & -I \end{bmatrix} \begin{Bmatrix} P^S \\ P^A \end{Bmatrix} \quad (3)$$

This decomposition principle applies if the vector components on the left hand side are expressed in a mirror image coordinate system. The force-displacement relations are thus expressed in symmetric coordinates as follows:

$$\begin{aligned} [K] \{U^S\} &= \{P^S\} \\ [K] \{U^A\} &= \{P^A\} \end{aligned} \quad (4)$$

The compatibility constraints are:

$$\begin{aligned} \{U^S{}_b\} &= \{0\} \\ \{U^A{}_b\} &= \{0\} \end{aligned} \quad (5)$$

Note that the boundary compatibility, when expressed in symmetric coordinates, does not cause coordinate coupling. One can also apply static reduction before or after the constraint relations, leaving in the a-set only boundary nodes other than nodes on the plane of symmetry.

$$\begin{aligned} [K_{aa}{}^S] \{U_a{}^S\} &= \{P_a{}^A\} \\ [K_{aa}{}^A] \{U_a{}^A\} &= \{P_a{}^A\} \end{aligned} \quad (6)$$

where K_{aa}^{S} and P_{a}^{S} are obtained from K and P^{S} (also K_{aa}^{A}, P_{a}^{A} from K and P^{A}) as follows:

$$[K_{aa}] = [\bar{K}_{aa}] + [K_{oa}]^{T} [G_{o}] \tag{7}$$

$$[G_{o}] = -[K_{oo}]^{-1} [K_{oa}] \tag{8}$$

$$\{P_{a}\} = \{\bar{P}_{a}\} + [G_{o}]^{T} \{P_{o}\} \tag{9}$$

$$\{U_{o}\} = [G_{o}] \{U_{a}\} + [K_{oo}]^{-1} \{P_{o}\} \tag{10}$$

The matrix reduction operations (5) - (10) are different between A and S components only insofar as to what they do with d.o.f.'s on the plane of symmetry: if such a d.o.f. is in the a-set for A-components, it will be in the o-set for S-components, and vice-versa.

3. STATIC REDUCTION USING SYMMETRY PRINCIPLES

Let us transform eqn. (6) back to physical coordinates using (2) and (3):

$$\frac{1}{2}\left[\begin{array}{c|c} K_{aa}^{S} + K_{aa}^{A} & K_{aa}^{S} - K_{aa}^{A} \\ \hline K_{aa}^{S} - K_{aa}^{A} & K_{aa}^{S} + K_{aa}^{A} \end{array}\right] \left\{\begin{array}{c} U_{a}^{R} \\ \hline U_{a}^{L} \end{array}\right\} = \frac{1}{2}\left\{\begin{array}{c} P_{a}^{R} + P_{a}^{L} \\ \hline P_{a}^{R} - P_{a}^{L} \end{array}\right\} \tag{11}$$

Physically interpreted, eqn. (11) represents the boundary stiffness equation of a substructure with dihedral symmetry.

The boundary d.o.f.'s occur in symmetric pairs. Eqn. (11) can be considered to be the end product of Phase I substructuring; the advantage of (11) is that it need not contain any a-set d.o.f.'s on the plane of symmetry, only nodes at boundaries with other substructures.

Data recovery in Phase III substructuring involves transforming the boundary displacement vectors to symmetric coordinates, then solving for the dependent displacements in symmetric coordinates.

$$\begin{Bmatrix} U_a^S \\ U_a^S \end{Bmatrix} = \begin{bmatrix} I & I \\ I & -I \end{bmatrix} \begin{Bmatrix} U_a^R \\ U_a^L \end{Bmatrix} \tag{12}$$

$$\{U_o^S\} = [G_o^S]\{U_a^S\} + [K_{oo}^S]^{-1}\{P_o^S\} \tag{13}$$

$$\{U_o^A\} = [G_o^A]\{U_a^A\} + [K_{oo}^A]^{-1}\{P_o^A\}$$

and transformation back to physical coordinates. Finally stresses and reaction forces are obtained in the right and left half-segments.

4. CONCLUSIONS

Two examples were presented to illustrate the combined application of static reduction and symmetry transformation to large finite element models. In the first example, the double stiffness reduction preceded symmetry tranformations; in the second example, the stiffness reduction took place after the introduction of symmetric components.

For mirror-image substructures having a large percentage of their nodes on the plane of symmetry, a new reduction scheme was presented. By taking into account the properties of symmetric components, this scheme offers significant cost savings over the NASTRAN's present "mirror image substructuring" technique. The structure in Figure 3 was used for comparison purposes: problem parameters are shown in Table 1; relative cost estimates appear in Table 2.

REFERENCES

1. MSC/NASTRAN User's Manual, 1978 Edition, by the MacNeal-Schwendler Corp.

2. MSC/NASTRAN Applications Manual, January 1979 Update, by the MacNeal-Schwendler Corp.

3. "Cormorant A Platform - New Roof Global Static Analysis," GSIE Report, March 9, 1976.

4. "Static Reduction of Substructures Satisfying Reflective Symmetry," by P. Fallet and A. Mera, NASTRAN User's Conference, Munich, April 27-28, 1977.

ACKNOWLEDGMENT

The ideas presented and the examples illustrated in this report are drawn in part on work performed by the author in the services of GSIE, Paris, France, in the period September 1975 - April 1977.

Fig. 1   Deepwater gravity platform: general view

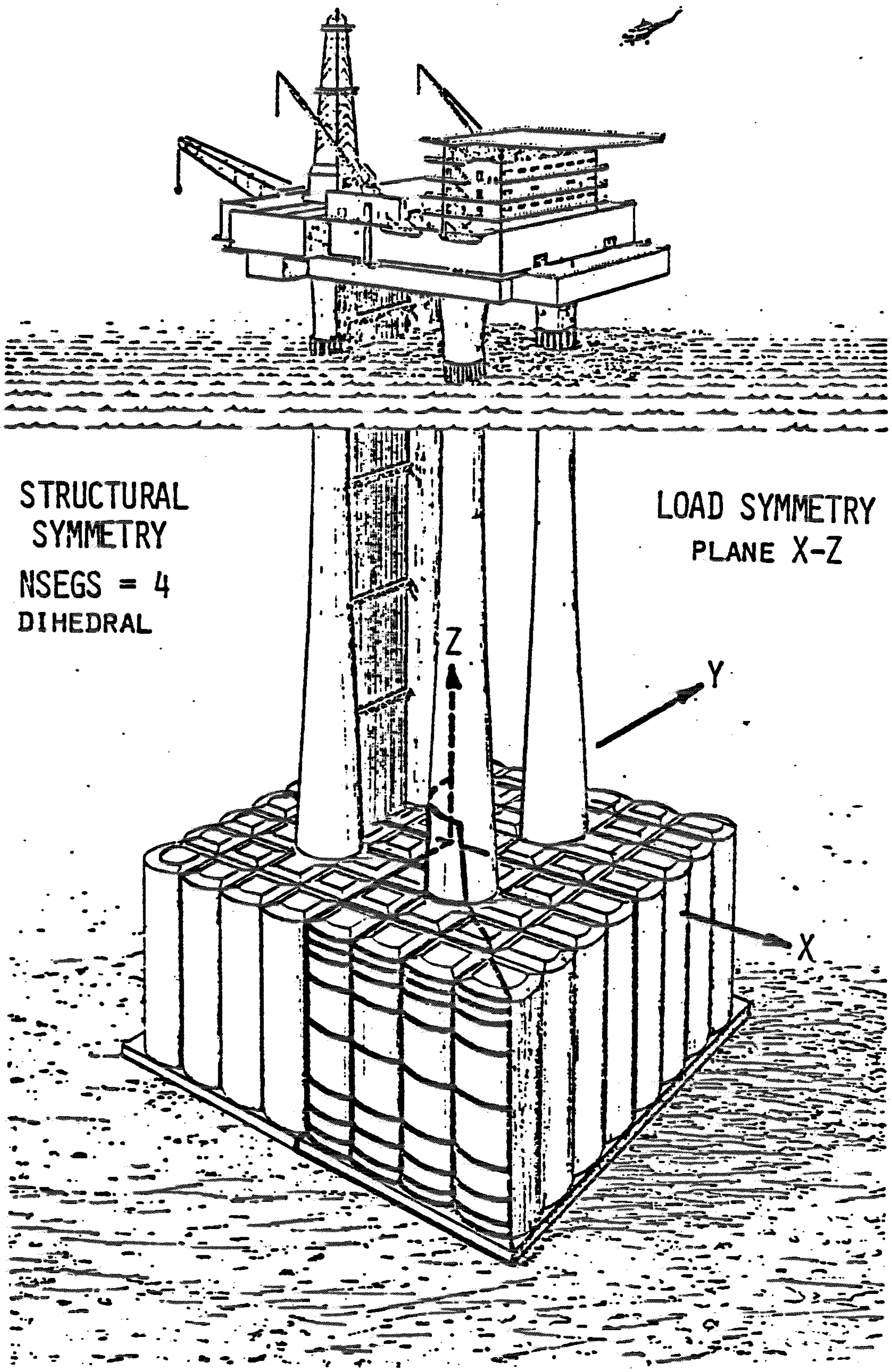

Fig. 2 Deepwater gravity platform: finite element model of a typical caisson segment

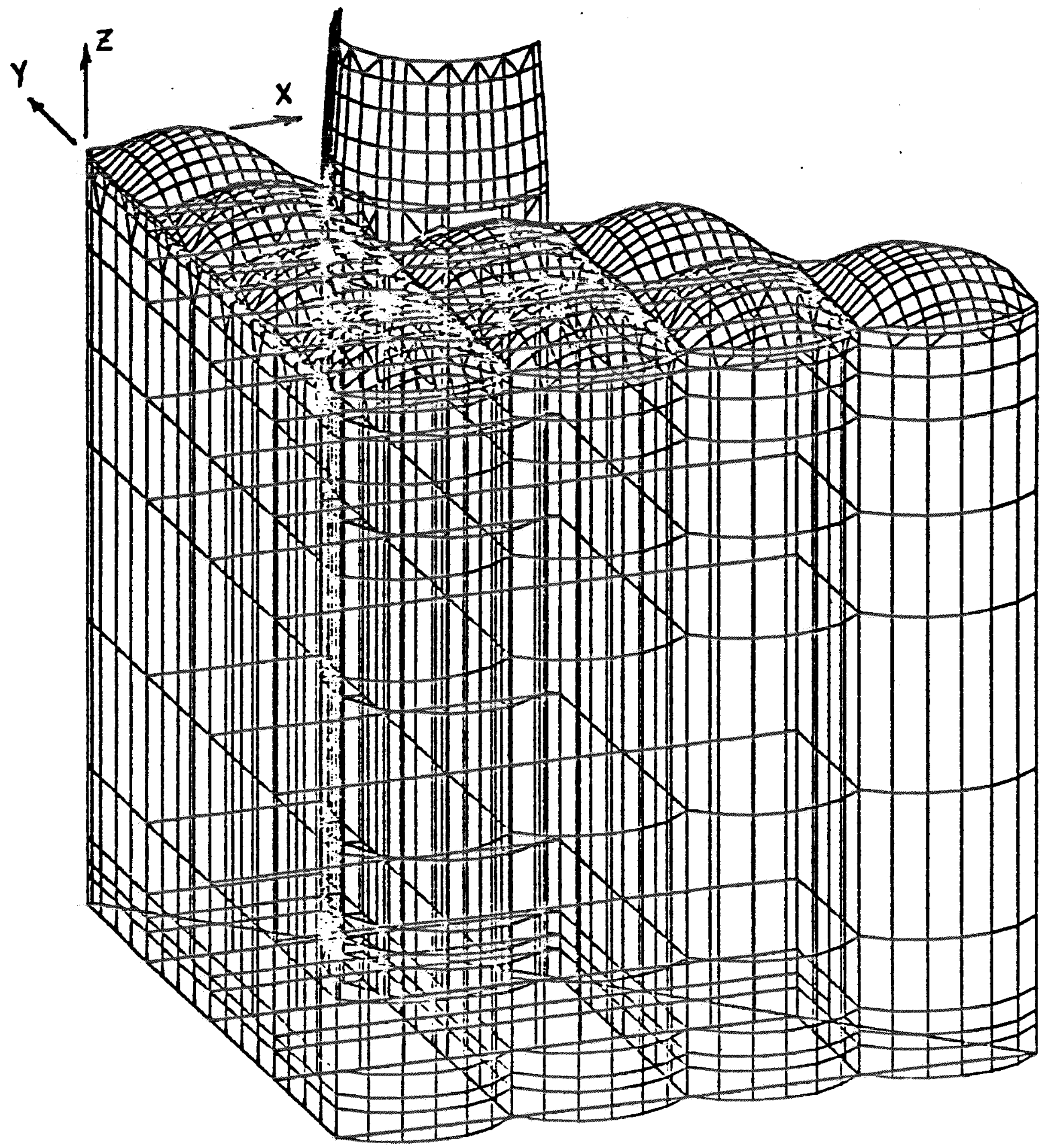

Fig. 3 Structure with dihedral substructures

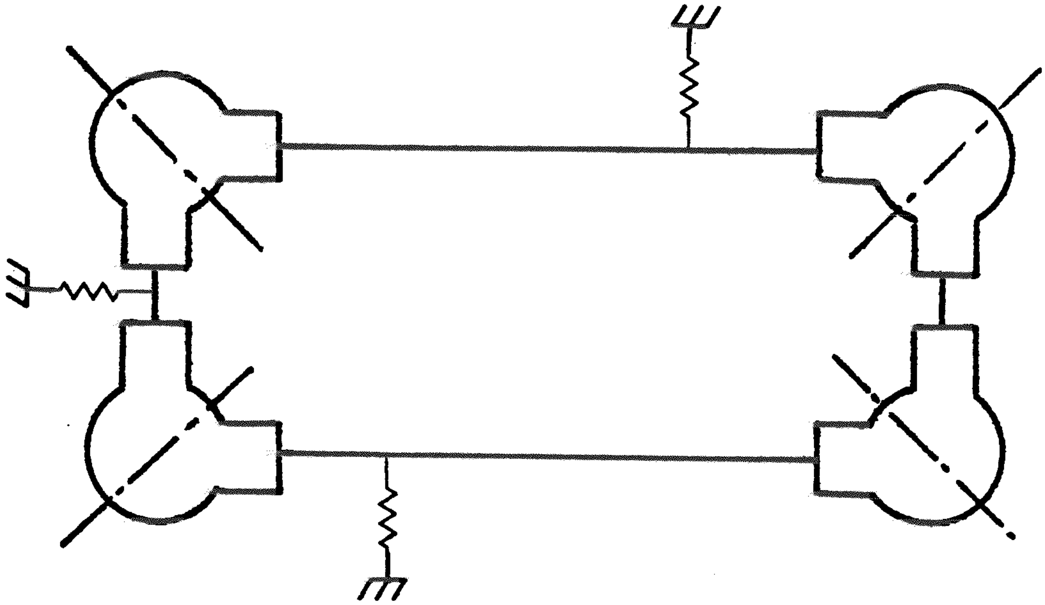

a. Global view

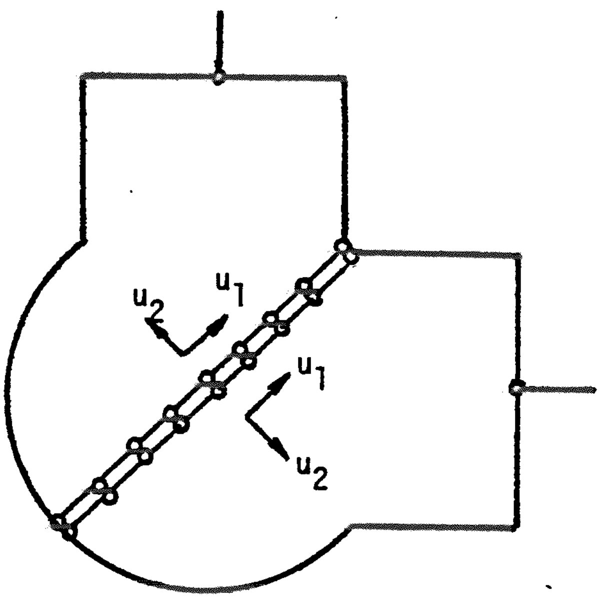

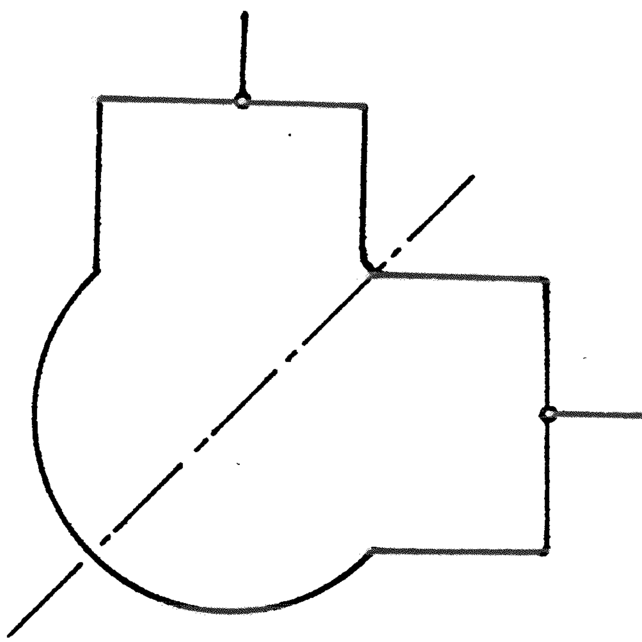

b. Two identical substructures in mirror-image coordinates. Circles denote boundary nodes after stiffness reduction.

c. Stiffness reduction to two boundary nodes using symmetry transform.

TABLE 1. PROBLEM SIZE PARAMETERS

1/2 SYMMETRIC SEGMENT

N_g = 654 nodes x 6 d.o.f./node

(of which 90 nodes are on the plane of symmetry and 3 nodes are on the boundary)

SUBSTRUCTURE WITH DIHEDRAL SYMMETRY

N_g = 1128 nodes x 6

N_a = 4 nodes x 6

RESIDUAL SUBSTRUCTURE

N_a = 76 nodes x 6

TOTAL FOR 4 SUBSTRUCTURES + RESIDUAL SUBSTRUCTURE

4582 nodes

TABLE 2. TIMING COMPARISONS FOR MAJOR MATRIX OPERATIONS

MIRROR-IMAGE SUBSTRUCTURING

Ph. I	Eliminate 562 internal nodes	
	DECOMP K_{oo}	1,950
	FBS $/G_o$	8,100
Ph. II	Solution of red. matrix, size 430 nodes	
	DECOMP K_{aa}	6,400
Ph. III	Dependent Data recovery	3,550
	TOTAL	20,000

NEW METHOD WITH DIHEDRAL SUBSTRUCTURES

Ph. I	Eliminate 651 internal nodes	
	DECOMP K_{oo}^S	2,470
	FBS $/G_o^S$	3,100
	DECOMP K_{oo}^A	2,470
	FBS $/G_o^A$	3,100
Ph. II	Solution of red. matrix, size 94 nodes	300
Ph. III	Dependent Data recovery	4,520
	TOTAL	16,000

NOTE: The timing figures are given in CPU-seconds.

APPENDIX - LIST OF SYMBOLS

Matrices:

K - stiffness matrix

U - displacement vector

P - load vector

G - transformation matrix

I - identity matrix

Subscripts:

a - analysis set

b - boundary set

o - omitted internal d.o.f.'s

Superscripts:

R/L - right/left half-segment (physical coordinates)

S/A - symmetric/antisymmetric components (transformed coordinates)